

1 **Coadministration of Antigen-conjugated and Free CpG: Effects of *in Vitro* and *in Vivo***
2 **Interactions in a Murine Model**

3

4 Melinda Herbáth^{a,*}, Zsuzsanna Szekeres^b, Dorottya Kövesdi^a, Krisztián Papp^b, Anna Erdei^{a,b},
5 József Prechl^b

6

7 ^a Department of Immunology, Eötvös Loránd University, 1/C Pázmány Péter sétány,
8 Budapest, 1117 Hungary

9 ^b Immunology Research Group of Hungarian Academy of Sciences, 1/C Pázmány Péter
10 sétány, Budapest, 1117 Hungary

11 * Corresponding author at Eötvös Loránd University, Department of Immunology, 1/C
12 Pázmány Péter sétány, Budapest, 1117 Hungary. Tel.: +36-1-3812175; Fax: +36-1-3812176;
13 E-mail: melinda.herbath@gmail.com

14

15 **Abbreviations:**

16 APC, antigen-presenting cell

17 ASC, antibody-secreting cell

18 BMDC, bone marrow-derived dendritic cell

19 CpG, cytosine guanine dinucleotide-containing unmethylated DNA motif (in this study: ODN
20 1668)

21 CTRL, control oligonucleotide (in this study: ODN 1720)

22 GM-CSF, granulocyte-macrophage colony-stimulating factor

23 IFA, incomplete Freund's adjuvant;

24 INH, TLR9 antagonist oligonucleotide (in this study: ODN 2088)

25 LN, lymph node

- 26 MycHH, a peptide construct consisting of a Myc tag and a HexaHistidine tag, that is
- 27 biotinylated on the N terminus;
- 28 ODN, oligodeoxynucleotide;
- 29 PS, phosphorothioate
- 30 RFI, relative fluorescence intensity
- 31 RU, relative unit
- 32 SA, streptavidin
- 33

34 **Abstract**

35

36 CpG oligodeoxynucleotides (CpG) are widely studied as promising adjuvants in vaccines
37 against a range of diseases including infection, cancer or allergy. Conjugating antigen to CpG
38 has been shown to potentiate the adjuvant effect via enhancing antigen uptake and danger
39 signaling by the very same cell. In the present study, using biotinylated CpG and streptavidin
40 as a model system, we demonstrate that CpG motif containing free and antigen-conjugated
41 oligonucleotides do not compete in terms of cell activation via TLR9, but do compete for
42 cellular uptake. Antigen-conjugated CpG enhances cellular association and uptake of the
43 antigen by antigen-presenting cells (APC) and T cells. Free CpG efficiently competes with
44 antigen-CpG conjugates in BMDC and T cells, but shows weak or no competition in B cells
45 that have higher TLR9 expression. Vaccination with antigen-conjugated CpG or with a
46 mixture of antigen and CpG elevates the level of antigen-specific antibodies but co-
47 administration of CpG-antigen conjugates and free CpG adversely effects immunogenicity.
48 These observations may help optimize CpG-based vaccine formulation.

49

50

51

52 **Keywords:** Antigen Presentation, Cell Activation, Vaccination, TLR9, CpG, Adjuvant

53

54 **1. Introduction**

55

56 Designing vaccines against infectious diseases, allergy or cancer with adjuvants is a central
57 issue nowadays. The route of administration, the formulation and the type of the adjuvant can
58 fundamentally determine the outcome of the immune response.

59 CpG motifs interact with TLR9 in the endolysosomal compartment from which host DNA is
60 usually excluded and this ligand binding occurs at a particular stage of endosome maturation
61 and acidification [1]. Interaction of TLR9 and its ligand stimulates an innate immune
62 response characterized by the production of cytokines, chemokines and immunoglobulins by
63 lymphocytes, macrophages, NK cells and DC [2-4]. In particular, the increased production of
64 IL-12 promotes IFN- γ production by NK cells and T cells, and enhances the antigen-specific
65 T cell proliferation and differentiation of naïve T cells towards the Th1 phenotype [5]. Most
66 of the researchers have focused on the cellular activating effect of the signal transduction
67 events that are triggered by TLR9 ligation while less is known about the modulation of
68 antigen uptake by CpG ODN. Some authors mentioned the relevance of 'stickiness' of
69 synthetic ODNs [6,7] that can take part in the uptake of antigen and thus have an impact on
70 the elicited immune response. There is evidence that ligation of CpG to a particulate antigen
71 can enhance the uptake of CpG via endocytosis initiated by the antigen-specific BCR [8].
72 However, when a non-specific B cell or other APC encounters a CpG-antigen conjugate –
73 which is probably a more common event in a physiological situation – has not been studied
74 widely. Only indirect effects of CpG treatment on enhancement of microbe uptake by
75 macrophages [9] or of amyloid β 1-42 peptide by microglial cells [10] were reported.

76 We have developed a modular system for experimental vaccination based on streptavidin
77 (SA) as a model antigen and monobiotinylated targeting units. Previously we used

78 enzymatically biotinylated single-chain Ab fragments and studied the effect of vaccination by
79 targeting model antigens to various receptors on murine APC, such as CR1/2, FcγRII/III or
80 CD40 [11-13]. Here we describe the effects of targeting our model antigen, SA, to TLR9
81 using synthetic CpG oligonucleotide ligands. Unmethylated bacterial DNA fragments,
82 containing CpG motifs are the ligands of the pattern recognition receptor TLR9, and these
83 ligands are widely investigated as potential molecular adjuvants. In this paper we report
84 competition studies on CpG-mediated antigen uptake and immune response modulation,
85 which strengthen the view that CpG-conjugated antigen is taken up preferentially in a
86 receptor-mediated fashion.

87 **2. Materials and Methods**

88

89 *2.1. Ethics Statement*

90

91 All the treatments of animals (mice) in this research followed the guidelines of the
92 Institutional Animal Care and Ethics Committee at Eötvös Loránd University that operated in
93 accordance with permissions 22.1/828/003/2007 issued by the Central Agricultural Office,
94 Hungary and all animal work was approved by the appropriate committee.

95

96 *2.2. Animals and cell culturing*

97

98 Six week old female BALB/c mice were purchased from Charles River Laboratories and were
99 housed under specific pathogen free conditions. Cells were cultured in medium RPMI 1640
100 (GIBCO - Invitrogen, Carlsbad, CA, US) supplemented with 5% heat-inactivated FCS
101 (GIBCO) in the case of spleen cells and supplemented with 10% heat-inactivated FCS in the
102 case of BMDC, 2 mM L-glutamine (Sigma–Aldrich, St. Louis, MO, US), 100 U/ml penicillin
103 (Sigma–Aldrich), 100 µg/ml streptomycin (Sigma–Aldrich), 50 µM 2-mercaptoethanol
104 (Sigma–Aldrich) and 1 mM sodium pyruvate (Reanal, Budapest, HU).

105

106 *2.3. CpG oligonucleotides*

107

108 All ODN had phosphorothioate (PS) linkages between the nucleic bases (marked with capital
109 letters), except between the last two 3' bases (marked with lowercase letters). ODN 1668
110 (CpG) (TCCATGACGTTCCCTGATGct) and biotinylated 1668
111 (TCCATGACGTTCCCTGATGct-biotin) ODN were purchased from Sigma-Aldrich; ODN

112 1720 (CTRL) (TCCATGAGCTTCCTGATGct), biotinylated 1720
113 (TCCATGAGCTTCCTGATGct-biotin), ODN 2088 (INH) (TCCTGGCGGGGAAGt) and
114 biotinylated 2088 (TCCTGGCGGGGAAGt-biotin) were obtained from Kromat Kft
115 (Budapest, HU). The PS backbone prevents ODN degradation.

116

117 2.4. *Generation of bone marrow-derived dendritic cells (BMDC)*

118

119 The principle method for generating BMDC with granulocyte-macrophage colony-stimulating
120 factor (GM-CSF) was adapted from a previous publication [14] with the following
121 modifications. BM was flushed from the femurs of BALB/c mice using a 21-gauge needle and
122 glucose–potassium–sodium (GKN) buffer. After Tris-ammonium chloride lysis of RBC, BM
123 cells were cultured in teflon bottles for 6 days at 37°C in 5% CO₂ humidified atmosphere at
124 10⁶ cells/ml in complete RPMI 1640 medium, supplemented with GM-CSF. Recombinant
125 murine GM-CSF concentration was adjusted to 34 ng/ml, based on ELISA (BD Biosciences,
126 Franklin Lakes, NJ, US) measurement of the supernatant of a murine GM-CSF producing
127 X63 mouse myeloma cell line (the kind gift of Zsuzsa Bajtay, ELTE, Budapest, HU).
128 According to the results of Zs. Bajtay, the usage of teflon bottles enhances the purity of the
129 BMDC culture from 80% to about 92% (unpublished data). The expanded BM culture was
130 incubated for one additional day without GM-CSF prior to further *in vitro* tests.

131

132 2.5. *In vitro cell activation*

133

134 Differentiated BMDC culture and freshly isolated spleen cells were plated onto 96 well plates
135 in 2×10⁵ and 10⁶ cells/well densities, respectively. Suboptimal activating doses of biotinylated
136 or free CpG were used (25 nM for spleen suspension and 50 nM for BMDC culture) with

137 equimolar amount of fluorescent SA (SA-Alexa Fluor 488, Invitrogen) and cells were
138 incubated for 1 day (spleen cells) or 2 days (BMDC culture) at 37°C in 5% CO₂ humidified
139 atmosphere.

140

141 2.6. *Flow cytometry*

142

143 Fluorescently labeled mAbs obtained from eBioscience (San Diego, CA, US) were the
144 following: anti-mouse CD45R-PerCP-Cy5.5 (clone: RA3-6B2), rat IgG2a-PerCP-Cy5.5
145 isotype control (clone: eBR2a), anti-mouse CD69-PE (clone: H1.2F3), armenian hamster IgG-
146 PE isotype control (clone: eBio299Arm), anti-mouse CD40-APC (clone: 1C10), rat IgG2a-
147 APC isotype control (clone: eBR2a); Rockland Immunochemicals (Gilbertsville, PA, US):
148 polyclonal IgG fraction of anti-Streptavidin (Rabbit); BD Biosciences (Franklin Lakes, New
149 Jersey, US): rat anti-mouse I-A/I-E-PE (clone: M5/114.15.2), rat IgG_{2b}, κ-PE isotype control.
150 Fluorescently labeled SA was purchased from Invitrogen (Carlsbad, CA, US). For cell surface
151 staining, cell suspensions were incubated on ice for 20 min with different combinations of
152 mAb, diluted in FACS buffer (PBS supplemented with 1% heat-inactivated FCS and 0.1%
153 sodium azide). Nonspecific binding was blocked using K9.361 Ab (ELTE, Department of
154 Immunology, Budapest, HU). After staining with fluorescently labeled mAb, cells were
155 washed and acquired by a FACSCalibur (BD Biosciences) flow cytometer and the results
156 were analyzed using FCSEXPRESS (De Novo Software). In the spleen cell suspension CD45R⁺
157 lymphocyte-sized cells were considered B cells and CD45R⁻ lymphocyte-sized cells were
158 considered T cells. In the BMDC suspension I-A/I-E⁺ cells were considered BMDC. Dead
159 cells were excluded on the basis of their light scattering properties. Anti-SA antibody was
160 used to detect cell-surface associated SA, whereas SA-fluorescence itself could be originated
161 from both the internal compartments of the cells and from the cell surface. Results of flow

162 cytometry (Fig. 2, Fig. 3 and SuppFig. 1) were expressed as relative fluorescence intensities
163 (RFI), which were calculated as follows. The geometric mean of fluorescence of a particular
164 cell population acquired after a given treatment was divided by the the geometric mean of
165 fluorescence acquired from the SA-treated control sample. $RFI = MFI_{(any\ treatment)} / MFI_{(SA}$
166 $treatment)$. Results of at least three independent experiments were summarized on the diagrams
167 of Fig. 2, Fig. 3 and SuppFig. 1.

168

169 2.7. *Immunization protocol*

170

171 The vaccine formulation contained equimolar complexes of 5 μ g (83.3 pmol) Streptavidin
172 (SA) (Sigma–Aldrich) and biotinylated synthetic, N-terminally biotinylated myc-his-tag
173 peptide (MycHH, sequence: biotin-SSSAAAEQKLISEE-DLNHHHHHH) (Sigma–Aldrich).
174 The SA-MycHH complex served as a model antigen in the immunizations. Biotinylated
175 and/or free CpG, CTRL or INH ODN were added to the SA-MycHH complex in equimolar
176 amounts.

177 For *in vivo* experiments, 8 female BALB/c mice per group (6-8 week old) were injected s.c.
178 into the hind footpads and the base of the tail with the treatments containing 5 μ g SA/mouse,
179 mixed with equal volume of Incomplete Freund’s adjuvant (IFA; Sigma-Aldrich) in a total
180 volume of 150 μ l/animal (Table 1, Fig. 1). A booster injection with the same concentration
181 and volume of adequate complexes was administered in IFA on day 14. Blood samples were
182 taken on day 0, 7, 21 and 28. Mice were sacrificed on day 28 and cells were isolated and
183 purified from the inguinal and popliteal lymph nodes (LN).

184

185 2.8. *ELISA*

186

187 Levels of antigen specific IgG1 and IgG2a were determined as described previously [12].
188 Briefly, 96-well plates were coated first with SA (Sigma–Aldrich) and then with biotinylated
189 MycHH peptide (Sigma–Aldrich). Following blocking, serial dilutions of sera of immunized
190 mice were measured into the wells in triplicates. Goat anti-mouse IgG1-HRP or goat anti-
191 mouse IgG2a-HRP (Southern Biotech, Birmingham, AL, USA) was used for detecting
192 antigen-specific antibodies. Relative concentrations were calculated using monoclonal mouse
193 anti-Myc-tag IgG1 (clone 9E10, Cell Signaling Technology, Danvers, MA, US) and mouse
194 anti-Myc-tag IgG2a (clone 9B11, Cell Signaling Technology) as standards. Results are
195 represented as relative units (RU).

196

197 2.9. *Reverse ELISPOT assay*

198

199 The number of antibody-secreting cells (ASC) in the draining LN after immunizations was
200 determined as described previously [13]. Briefly, 5×10^5 cells, isolated from draining LN of
201 immunized mice were incubated in quadruplicates for 20 h at 37°C. Plates were then washed
202 and incubated with SA-HRP (Sigma-Aldrich) conjugated to MycHH in equimolar amounts
203 (1.67 nM) at 37°C for 1 h. The spots were developed, the membranes were washed, dried and
204 scanned, and the number of spots was determined by the ImmunoSpot software (C.T.L.).

205

206 2.10. *Reverse Protein Microarray*

207

208 Sera from all immunized mice were spotted individually onto nitrocellulose-covered glass
209 slides using a BioOdyssey Calligrapher miniarrayer (Bio-Rad Laboratories, Hercules, CA,
210 US). Features were printed in triplicates of 1:5 dilutions then stored at 4 °C in sealed bags.
211 Dried arrays were rinsed in PBS for 15 min before use, and then blocked with PBS containing

212 5% BSA (Sigma-Aldrich) and 0.05% Tween 20 (BSA-PBS-Tween) for 30 min at RT.
213 Antigen complexes was prepared by conjugating SA-Alexa647 (Molecular Probes,
214 Invitrogen) to biotinylated MycHH peptide (Sigma–Aldrich) in 1:1 molar ratio and diluted
215 1:4000 in BSA-PBS-Tween. Labeling with the antigen (SA-MycHH complex) was conducted
216 at room temperature for 1 h in BSA-PBS-Tween. Following washing in PBS-Tween, arrays
217 were dried and scanned with an Axon GenePix 4300A scanner and data were analyzed with
218 GenePixPro 7 software (Molecular Devices). Relative fluorescence intensities (RFI) were
219 calculated by subtracting background fluorescence from the median of three parallel signal
220 intensities. Signals not exceeding two standard deviations of local background signals on a
221 slide were clamped to an arbitrary value of 1.

222

223 *2.11. MACS*

224

225 For gene expression studies differentiated BMDC were positively separated from the BM
226 culture with anti-mouse CD11c magnetic microbeads (Miltenyi Biotec, Bergisch Gladbach,
227 DE) according to the manufacturer's protocols. FcRs were blocked by naive BALB/c serum.
228 Activated spleen suspension was separated to CD19⁺ (B cell) and CD19⁻ (T cell) populations
229 with anti-mouse CD19 magnetic beads (Miltenyi Biotec). The purity of the resulting B and T
230 cell suspensions was at least 95%.

231

232 *2.12. Analysis of TLR9 gene expression by qPCR*

233 RNA was extracted from magnetically separated CD19 positive B cells, CD19 negative T
234 cells and CD11c positive BMDC using TRIzol reagent (Life Technologies, Carlsbad, CA,
235 US) and converted to cDNA for real-time PCR analysis as described previously [15]. Real-
236 time PCR was performed on an ABI PRISM 7000 Sequence Detection System (Applied

237 Biosystems). TLR9 mRNA was quantified using primers and FAM-labeled probes from
238 Applied Biosystems (Taqman assays on demand) according to the manufacturer's
239 instructions. Variations in cDNA input were normalized using $\beta 2m$ (Applied Biosystems) as a
240 reference gene and the expression level of TLR9 in B and T cells was calculated as the n -fold
241 difference relative to the expression found in BMDC.

242

243 2.13. *Statistical analysis*

244 Regarding *in vitro* experiments, all data were normalized to the data of SA treatment and
245 statistical differences were assessed by pairwise comparisons of relevant groups using
246 permutation tests with the help of the software R. Briefly, values from the groups to be
247 compared were randomly reassigned to two groups and the difference between the group
248 means was calculated. Distribution of 5000 randomizations was drawn and the two-tailed p
249 value corresponding to the real sample assignments was determined. The arithmetic mean of
250 50 such p values was accepted as the probability of α -error. Values of $p < 0.05$ were
251 considered significant and were indicated as follows: * $p < 0.05$; ** $p < 0.01$; *** $p < 0.001$.
252 Statistical differences between the control and the experimental immunization groups were
253 determined by nonparametric, Kruskal-Wallis ANOVA analysis for ELISA and ELISPOT
254 and reverse protein array experiments, using Statistica 8 software (StatSoft). Quantitative data
255 are expressed as individual data of mice; the horizontal lines indicate medians of the groups.
256 Levels of significance were indicated with asterisks as mentioned previously.

257 **3. Results**

258

259 *3.1. Antigen-conjugated CpG enhances cellular association and uptake of the antigen by*
260 *APC and T cells*

261

262 We characterized the efficiency of antigen capture and uptake using fluorescently labeled SA.
263 Synthetic biotinylated CpG (ODN 1668) was mixed with SA in a 1:1 ratio and coincubated
264 with bone marrow-derived dendritic cells (BMDC), and splenocyte suspension. B220 positive
265 splenocytes were referred to as B cells, and B220 negative splenocytes were referred to as T
266 cells. Conjugating CpG to the protein antigen resulted in enhanced association to B and T
267 lymphocytes and BMDC after 24 h of incubation (Fig. 2). To exclude that increased
268 fluorescence was a result of SA-CpG sticking to the cell surface, SA accessibility was
269 assessed by anti-SA antibodies. Weak or missing anti-SA signals indicated that cellular
270 uptake was mainly responsible for CpG-mediated SA association to the cells (Fig. 2). The
271 level of APC activation was low because the doses of CpG used here were titrated to be
272 suboptimal to allow modulation in the following competition studies. There was no difference
273 between the activatory potential of SA + CpG and SA-CpG treatments (Fig. 2).

274

275 *3.2. Non-biotinylated excess CpG efficiently competes with CpG-antigen conjugates on*
276 *BMDC and T cells, but shows weak or no competition on B cells*

277

278 In order to prove that the increase in uptake of SA-CpG complexes compared to the uptake of
279 SA alone is due to a receptor-mediated and therefore a saturable process we tested the effects
280 of free CpG and other types of ODN on the SA-CpG uptake. In the presence of a 100-fold
281 molar excess of free CpG, association of SA-CpG complexes to T cells and BMDC was

282 robustly reduced. In contrast, the SA-CpG uptake of B lymphocytes could not be inhibited
283 even with a 100-fold excess of free CpG (Fig. 3A).

284 Although the addition of excess CpG resulted in enhanced B cell and BMDC activation, the
285 difference between association of SA-CpG to the different cell types was not a consequence
286 of the strong activation of B cells, since the same results were observed with excess CTRL
287 (ODN 1720) that has little or no activating effect (Fig. 3B). A TLR9 inhibitor ODN, marked
288 INH (ODN 2088) showed competition with SA-CpG in the case of all three cell types though
289 with less efficiency (Fig. 3C). The addition of excess ODN had no effect on SA accessibility
290 on the cell surface (Supplementary Fig. 1A–C), except in the case of B cells treated with SA-
291 CpG + INH in 100-fold excess. In this last case the inhibitory ODN also competed with the
292 low amounts of cell surface bound SA-CpG complexes (Supplementary Fig. 1C).

293 As the weak competition between free and antigen-conjugated CpG in B cells could not be
294 explained by the activatory effect of excess CpG, we performed RT-PCR measurements to
295 compare the expression of TLR9 in these cell types. Both in untreated and activated B cells,
296 the expression of TLR9 was much higher compared to BMDC or T cells (Supplementary Fig.
297 2A-B), suggesting that saturation of the receptor would be more difficult to achieve in these
298 cells.

299

300 *3.3. CpG conjugation to SA elevates the level of antigen-specific antibodies*

301

302 As we found that CpG facilitates the accumulation of a CpG-conjugated protein in DC and
303 this can be inhibited by free CpG, the question arose, whether this phenomenon would occur
304 *in vivo*. To test this hypothesis we vaccinated mice with four different formulations of a SA-
305 peptide complex with CpG or other ODN. The biotinylated c-myc-HexaHistidine tag peptide
306 (MycHH) that was conjugated to SA in equimolar ratio served as a positive control epitope

307 during serological detection. The peptide content is not indicated separately to simplify the
308 nomination of the vaccine formulations that are summarized in Table 1 and Fig. 1. SA was
309 administered in itself (SA), together with non-biotinylated free CpG (SA + CpG); together
310 with biotinylated CpG to form complexes (SA-CpG) and together with a 1:1 mixture of
311 nonbiotinylated and biotinylated CpG (SA-CpG + CpG). For the last group the amount of free
312 and biotinylated CpG together was equal to the CpG amount of the other groups. IFA was
313 used to ensure the development of an immune response since relatively low amount of CpG
314 was used (83 pmol/mice/injection). We used suboptimal CpG doses to be able to modulate the
315 immune response and in order to avoid systemic responses caused by high-dose soluble CpG.
316 First, we compared the effect of the conjugation of biotinylated forms of the different ODN
317 used in the *in vitro* experiments (CpG, CTRL or INH) to the model antigen SA. Conjugation
318 of antigen to CpG, but not to the other two types of ODN, elevated the level of antigen-
319 specific antibodies (Fig. 4A). At this dosage only conjugated but not free CpG had
320 statistically significant immune response enhancing effect, as shown by reverse array (Fig.
321 4B), ELISA (Fig. 5A-B) and ELISPOT (Fig. 6).

322

323 3.4. *Free CpG adversely influences the adjuvant effect of antigen-CpG conjugation*

324

325 To study the *in vivo* interactions between free CpG and SA-CpG complexes, we prepared a
326 formulation where half of the CpG was conjugated to SA, and half of it was in free form.
327 Interestingly, instead of showing an additive effect, vaccination with the SA-CpG + CpG
328 formulation did not enhance immune responses at all (Fig. 4B - Fig. 6). Antigen-specific Ab
329 levels (Fig. 4B, 5B) and the number of Ab secreting cells (Fig. 6) were comparable to the SA
330 group where no CpG was present, and were significantly lower compared to the SA-CpG
331 group.

332 **4. Discussion**

333

334 TLR9 is recognized as the primary receptor for unmethylated bacterial CpG DNA, which
335 triggers signaling and gene transcription upon binding to TLR9 in the endosomes. Here we
336 showed that a protein antigen efficiently accumulates in different leukocytes when it is linked
337 to a TLR9 ligand, a single-stranded phosphorothioate-protected (PS) CpG ODN. The
338 mechanism of CpG uptake is controversial, as non-specific internalization [16] as well as
339 specific uptake mechanisms have been suggested. Various receptors and transfer molecules
340 came into view as potential CpG binders, like CD14 [17], membrane bound scavenger
341 receptors like CXCL16 [18] or SR-A and MARCO [19], DEC-205 [20], human CR2 [21], the
342 KIR3DL2 receptor on human NK cells [22], and alpha 2-macroglobulin [23]. It has also been
343 proposed that the uptake of ODN that have a PS backbone differs from that of natural
344 phosphodiester backboned ODN, and PS ODN bind to many proteins due to nonspecific
345 interactions [24]. The number of these - sometimes controversial - studies shows that there is
346 much to be done to elucidate the uptake mechanisms of CpG ODN or its synthetic analogues
347 and to better understand the intracellular fate and mechanism of effect of complexes that
348 consist of protein antigen and CpG. Whatever the internalization mechanism could be, our
349 results point to a TLR9-mediated accumulation that can be saturated in cells where TLR9
350 expression is low. Of the two APC types we studied, splenic B-cells showed more than ten
351 times higher expression of TLR9 compared to BMDC (Supplementary Fig. 2,
352 www.immgen.org, 2013). Splenic T cells also express TLR9 at low levels, which delivers
353 costimulatory signals for TCR-induced activation [25]. About tenfold increase in fluorescence
354 signal was observed, when cells were incubated with fluorescent SA conjugated with CpG
355 (SA-CpG), compared to the incubation with a SA + CpG mixture. In the case of B cells part
356 of the SA-fluorescence originated from the surface of the cells, as SA was detected by anti-

357 SA antibodies (Fig. 2). Thus, the extent of SA-CpG accumulation was not proportional to
358 TLR9 expression, indicating that other factors limited maximal accumulation. On the other
359 hand, competition experiments were in agreement with TLR9 expression levels: higher
360 amounts of free ODN were required to inhibit SA accumulation by B cells. ODN with PS
361 backbone have been shown to compete for TLR9 binding [26], explaining the competitive
362 effect of CTRL and INH (Fig. 3). Taken together these results suggest that TLR9 retains
363 CpG-conjugated SA within the cells.

364

365 Antigen-conjugated CpG activated APC, such as B cells and DC, but not T cells. These
366 results are in line with previous works showing that in contrast to APC that are activated by
367 CpG stimulus alone [27], naive T cells need additional TCR ligation to be able to react to
368 CpG stimuli, reviewed in [28]. Moreover, Landrigan *et. al.* showed that this costimulating
369 effect of different ODN on T cells occurs independently of TLR9 and MyD88, and TLR9
370 antagonists can also promote costimulation of anti-CD3 treated CD4⁺ T cells [25].

371

372 Our immunization studies suggest that instead of showing additive immunostimulatory
373 properties, antigen-conjugated and free CpG rather cancel out each other's effects. Both the
374 number of antigen-specific ASC and the circulating Ab levels were comparable to
375 immunizations with SA alone, and were significantly weaker than the SA-CpG induced
376 effects (Fig. 4-6). We speculate that competition between SA-CpG complexes and free CpG
377 occurs in DC *in vivo*, resulting in poorer antigen uptake or accumulation by these cells.
378 The amounts of CpG and antigen we used for immunizations (83.3 pmol/mouse) were set to
379 be close to the minimum concentration that was needed to trigger cell activation *in vitro* (5
380 pmol for 10⁶ spleen cells or 10 pmol for 2×10⁵ BMDC). By comparison, in other vaccination
381 studies where the aim was to elicit a strong immune response against the injected antigen,

382 orders of magnitude higher amounts of CpG were used [29-31]. In contrast to these studies,
383 the concentration we used might be rather suitable for monitoring subtle differences between
384 the immunomodulating effects of immunization with materials of similar composition but
385 different formulation. Our purpose was also to avoid systemic reactions known to be induced
386 by high amounts of soluble CpG [32,33].

387

388 In conclusion, beside the direct activating effect of CpG exerted on the target cells via TLR9,
389 CpG-coupled antigens also show improved cellular uptake, which could contribute to the
390 enhanced immune response against such conjugates. The identity of the receptor responsible
391 for improved cellular uptake remains to be confirmed; nevertheless competition between free
392 CpG and CpG coupled to antigen reduces the amount of antigen that accumulates in the target
393 cells. Thus, surplus free CpG can even hinder rather than promote the effects of CpG-coupled
394 antigens when these are used at concentrations relevant for modeling human vaccination.

395 **Funding**

396

397 These studies were funded by the NKTH-OTKA K109683 grant to József Prechl. The
398 European Union and the European Social Fund have provided financial support to the project
399 under the grant agreement no. TÁMOP 4.2.1./B-09/1/KMR-2010-0003. The financial support
400 of the Hungarian Academy of Sciences is gratefully acknowledged. Krisztián Papp is
401 supported by the János Bolyai Research Scholarship of the Hungarian Academy of Sciences.
402 Dorottya Kövesdi's work was supported by the European Union and the State of Hungary, co-
403 financed by the European Social Fund in the framework of TÁMOP 4.2.4. A/1-11-1-2012-
404 0001 "National Excellence Program". The research was supported by the Hungarian
405 Scientific Research Fund (OTKA-NK 104846).

406 **Acknowledgements**

407

408 We thank Andrea Balogh for her critical comments on the manuscript and Árpád Mikesy and

409 Katalin Paréj for the technical assistance.

410

411 **References**

412

- 413 [1] Ahmad-Nejad P, Hacker H, Rutz M, Bauer S, Vabulas RM, Wagner H. Bacterial
414 CpG-DNA and lipopolysaccharides activate Toll-like receptors at distinct cellular
415 compartments. *Eur J Immunol* 2002;32:1958-1968.
- 416 [2] Krieg AM, Yi AK, Matson S, Waldschmidt TJ, Bishop GA, Teasdale R, et al. CpG
417 motifs in bacterial DNA trigger direct B-cell activation. *Nature* 1995;374:546-549.
- 418 [3] Stacey KJ, Sweet MJ, Hume DA. Macrophages ingest and are activated by bacterial
419 DNA. *J Immunol* 1996;157:2116-2122.
- 420 [4] Ballas ZK, Rasmussen WL, Krieg AM. Induction of NK activity in murine and human
421 cells by CpG motifs in oligodeoxynucleotides and bacterial DNA. *J Immunol*
422 1996;157:1840-1845.
- 423 [5] Krieg AM. CpG motifs in bacterial DNA and their immune effects. *Annu Rev*
424 *Immunol* 2002;20:709-760.
- 425 [6] Zhao Q, Matson S, Herrera CJ, Fisher E, Yu H, Krieg AM. Comparison of cellular
426 binding and uptake of antisense phosphodiester, phosphorothioate, and mixed
427 phosphorothioate and methylphosphonate oligonucleotides. *Antisense research and*
428 *development* 1993;3:53-66.
- 429 [7] Brown DA, Kang SH, Gryaznov SM, DeDionisio L, Heidenreich O, Sullivan S, et al.
430 Effect of phosphorothioate modification of oligodeoxynucleotides on specific protein
431 binding. *J Biol Chem* 1994;269:26801-26805.
- 432 [8] Eckl-Dorna J, Batista FD. BCR-mediated uptake of antigen linked to TLR9 ligand
433 stimulates B-cell proliferation and antigen-specific plasma cell formation. *Blood*
434 2009;113:3969-3977.
- 435 [9] Utaisinchaoen P, Kespichayawattana W, Anuntagool N, Chaisuriya P, Pichyangkul S,
436 Krieg AM, et al. CpG ODN enhances uptake of bacteria by mouse macrophages. *Clin*
437 *Exp Immunol* 2003;132:70-75.
- 438 [10] Iribarren P, Chen K, Hu J, Gong W, Cho EH, Lockett S, et al. CpG-containing
439 oligodeoxynucleotide promotes microglial cell uptake of amyloid beta 1-42 peptide by
440 up-regulating the expression of the G-protein- coupled receptor mFPR2. *FASEB J*
441 2005;19:2032-2034.
- 442 [11] Prechl J, Molnar E, Szekeres Z, Isaak A, Papp K, Balogh P, et al. Murine CR1/2
443 targeted antigenized single-chain antibody fragments induce transient low affinity
444 antibodies and negatively influence an ongoing immune response. *Adv Exp Med Biol*
445 2007;598:214-225.
- 446 [12] Szekeres Z, Herbath M, Angyal A, Szittner Z, Virag V, Balogh P, et al. Modulation of
447 immune response by combined targeting of complement receptors and low-affinity
448 Fcγ receptors. *Immunol Lett* 2010;130:66-73.
- 449 [13] Szekeres Z, Herbath M, Szittner Z, Papp K, Erdei A, Prechl J. Modulation of the
450 humoral immune response by targeting CD40 and FcγR2/3; delivery of
451 soluble but not particulate antigen to CD40 enhances antibody responses with a Th1
452 bias. *Mol Immunol* 2011;49:155-162.
- 453 [14] Inaba K, Inaba M, Romani N, Aya H, Deguchi M, Ikehara S, et al. Generation of large
454 numbers of dendritic cells from mouse bone marrow cultures supplemented with
455 granulocyte/macrophage colony-stimulating factor. *J Exp Med* 1992;176:1693-1702.
- 456 [15] Janas ML, Groves P, Kienzle N, Kelso A. IL-2 regulates perforin and granzyme gene
457 expression in CD8+ T cells independently of its effects on survival and proliferation. *J*
458 *Immunol* 2005;175:8003-8010.

- 459 [16] Hacker H, Mischak H, Miethke T, Liptay S, Schmid R, Sparwasser T, et al. CpG-
460 DNA-specific activation of antigen-presenting cells requires stress kinase activity and
461 is preceded by non-specific endocytosis and endosomal maturation. *EMBO J*
462 1998;17:6230-6240.
- 463 [17] Baumann CL, Aspalter IM, Sharif O, Pichlmair A, Bluml S, Grebien F, et al. CD14 is
464 a coreceptor of Toll-like receptors 7 and 9. *J Exp Med* 2010;207:2689-2701.
- 465 [18] Gursel M, Gursel I, Mostowski HS, Klinman DM. CXCL16 influences the nature and
466 specificity of CpG-induced immune activation. *J Immunol* 2006;177:1575-1580.
- 467 [19] Jozefowski S, Sulahian TH, Arredouani M, Kobzik L. Role of scavenger receptor
468 MARCO in macrophage responses to CpG oligodeoxynucleotides. *J Leukoc Biol*
469 2006;80:870-879.
- 470 [20] Lahoud MH, Ahmet F, Zhang JG, Meuter S, Policheni AN, Kitsoulis S, et al. DEC-
471 205 is a cell surface receptor for CpG oligonucleotides. *Proc Natl Acad Sci U S A*
472 2012;109:16270-16275.
- 473 [21] Asokan R, Banda NK, Szakonyi G, Chen XS, Holers VM. Human complement
474 receptor 2 (CR2/CD21) as a receptor for DNA: Implications for its roles in the
475 immune response and the pathogenesis of systemic lupus erythematosus (SLE). *Mol*
476 *Immunol* 2012;53:99-110.
- 477 [22] Sivori S, Falco M, Carlomagno S, Romeo E, Soldani C, Bensussan A, et al. A novel
478 KIR-associated function: evidence that CpG DNA uptake and shuttling to early
479 endosomes is mediated by KIR3DL2. *Blood* 2010;116:1637-1647.
- 480 [23] Anderson RB, Cianciolo GJ, Kennedy MN, Pizzo SV. Alpha 2-macroglobulin binds
481 CpG oligodeoxynucleotides and enhances their immunostimulatory properties by a
482 receptor-dependent mechanism. *J Leukoc Biol* 2008;83:381-392.
- 483 [24] Heeg K, Dalpke A, Peter M, Zimmermann S. Structural requirements for uptake and
484 recognition of CpG oligonucleotides. *Int J Med Microbiol* 2008;298:33-38.
- 485 [25] Landrigan A, Wong MT, Utz PJ. CpG and non-CpG oligodeoxynucleotides directly
486 costimulate mouse and human CD4+ T cells through a TLR9- and MyD88-
487 independent mechanism. *J Immunol* 2011;187:3033-3043.
- 488 [26] Avalos AM, Ploegh HL. Competition by inhibitory oligonucleotides prevents binding
489 of CpG to C-terminal TLR9. *Eur J Immunol* 2011;41:2820-2827.
- 490 [27] Hacker H, Vabulas RM, Takeuchi O, Hoshino K, Akira S, Wagner H. Immune cell
491 activation by bacterial CpG-DNA through myeloid differentiation marker 88 and
492 tumor necrosis factor receptor-associated factor (TRAF)6. *J Exp Med* 2000;192:595-
493 600.
- 494 [28] Kulkarni R, Behboudi S, Sharif S. Insights into the role of Toll-like receptors in
495 modulation of T cell responses. *Cell and tissue research* 2011;343:141-152.
- 496 [29] Oxenius A, Martinic MM, Hengartner H, Klenerman P. CpG-containing
497 oligonucleotides are efficient adjuvants for induction of protective antiviral immune
498 responses with T-cell peptide vaccines. *J Virol* 1999;73:4120-4126.
- 499 [30] Vabulas RM, Pircher H, Lipford GB, Hacker H, Wagner H. CpG-DNA activates in
500 vivo T cell epitope presenting dendritic cells to trigger protective antiviral cytotoxic T
501 cell responses. *J Immunol* 2000;164:2372-2378.
- 502 [31] Dalpke AH, Zimmermann S, Albrecht I, Heeg K. Phosphodiester CpG
503 oligonucleotides as adjuvants: polyguanosine runs enhance cellular uptake and
504 improve immunostimulative activity of phosphodiester CpG oligonucleotides in vitro
505 and in vivo. *Immunology* 2002;106:102-112.
- 506 [32] Sparwasser T, Miethke T, Lipford G, Borschert K, Hacker H, Heeg K, et al. Bacterial
507 DNA causes septic shock. *Nature* 1997;386:336-337.

508 [33] Heikenwalder M, Polymenidou M, Junt T, Sigurdson C, Wagner H, Akira S, et al.
509 Lymphoid follicle destruction and immunosuppression after repeated CpG
510 oligodeoxynucleotide administration. *Nat Med* 2004;10:187-192.
511
512

513 **Figure Legends**

514

515 **Figure 1. Composition of complexes and labeling of cells.**

516 Composition of complexes used for *in vitro* treatments and vaccines and the labeling of
517 BMDC and spleen cells for *in vitro* tests.

518

519 **Figure 2. Comparing the effects of free and antigen-conjugated CpG on antigen uptake
520 and cell activation.**

521 Total SA shows the association of labeled SA to either in- or outside of the cells, surface SA
522 shows the anti-SA staining of the complexes only on the cell surface. Activation is measured
523 by the detection of activation marker upregulation (CD40 on BMDC and CD69 on spleen cell
524 suspension). The concentration of the different treatments was 50 nM for BMDC and 25 nM
525 for spleen cells. Cells were harvested 24 h after stimulation and analyzed by flow cytometry.
526 CD45R⁺ lymphocyte-sized cells were considered B cells, CD45R⁻ lymphocyte-sized cells
527 were considered T cells, I-A/I-E⁺ cells were considered BMDC. The diagrams show mean +
528 SD of at least three independent experiments, normalized to the SA treatment. Statistical
529 differences were assessed by pairwise comparisons of SA + CpG and SA-CpG groups using
530 permutation tests, *p < 0.05; ***p < 0.001. RFI, relative fluorescence intensity.

531

532 **Figure 3. Comparing the effects of different excess ODN on the uptake of SA-CpG and
533 cell activation.**

534 Non-biotinylated CpG (A), CTRL (B) and INH (C) ODN were added in 10- and 100-fold
535 excess. Total SA shows the association of labeled SA to either in- or outside of the cells and
536 activation is measured by the detection of activation marker upregulation (CD40 on BMDC
537 and CD69 on spleen cell suspension). The concentration of SA-CpG was 50 nM for BMDC

538 and 25 nM for spleen cells. Cells were harvested 24 h after stimulation and analyzed by flow
539 cytometry. CD45R⁺ lymphocyte-sized cells were considered B cells, CD45R⁻ lymphocyte-
540 sized cells were considered T cells, I-A/I-E⁺ cells were considered BMDC. The diagrams
541 show mean + SD of at least three independent experiments, normalized to the SA treatment.
542 Statistical differences were assessed by pairwise comparisons of the SA-CpG treatment and
543 the treatments containing excess ODN, using permutation tests, *p < 0.05; **p < 0.01; ***p <
544 0.001. RFI, relative fluorescence intensity.

545

546 **Figure 4. Levels of antigen-specific total Ig on day 28 after immunization.**

547 Eight female BALB/c mice per group were injected s.c. into the hind footpads and the base of
548 the tail with equimolar SA complexes containing 5 µg SA/mouse, mixed with equal volume
549 of IFA, followed by a booster injection with the same treatments on day 14. Blood samples
550 were taken on day 28 and total levels of antigen-specific antibodies were assessed by reverse
551 protein microarray. Comparison of antigen-specific Ig levels following vaccination with
552 different ODN (CpG, CTRL or INH) conjugated to SA (A). Comparison of antigen-specific
553 Ig levels following vaccination with SA-conjugated and/or free CpG (B). Each dot represents
554 data obtained from one mouse and horizontal lines show the medians of the groups. Statistical
555 significance was calculated using a Kruskal-Wallis test (non parametric 1-way Anova), and a
556 Dunn's *post hoc* test. *p<0.05 and **p<0.01. RFI, relative fluorescence intensity.

557

558 **Figure 5. Concentration of antigen-specific IgG1 and IgG2a antibodies on day 28 after**
559 **immunization.**

560 Eight female BALB/c mice per group were injected s.c. into the hind footpads and the base of
561 the tail with equimolar SA complexes containing 5 µg SA/mouse, mixed with equal volume
562 of IFA, followed by a booster injection with the same treatments on day 14. Blood samples

563 were taken on day 28 and the levels of antigen-specific IgG1 (A) and IgG2a (B) antibodies
564 were measured by ELISA. Each dot represents data obtained from one mouse and horizontal
565 lines show the medians of the groups. Statistical significance was calculated using a Kruskal-
566 Wallis test (non parametric 1-way Anova), and a Dunn's *post hoc* test. ** $p < 0.01$. Results are
567 represented as relative units (RU).

568

569 **Figure 6. The numbers of antigen-specific ASC in the regional lymph nodes on day 28**
570 **after immunization.**

571 Eight female BALB/c mice per group were injected s.c. into the hind footpads and the base of
572 the tail with equimolar SA complexes containing 5 μg SA/mouse, mixed with equal volume
573 of IFA, followed by a booster injection with the same treatments on day 14. Mice were
574 sacrificed on day 28 and the number of antigen-specific ASC in the regional LN was assessed
575 by reverse ELISPOT. Results are represented as number of antigen-specific ASC/ 5×10^5 cells.
576 Each dot represents data obtained from one mouse and horizontal lines show the medians of
577 the groups. Statistical significance was calculated using a Kruskal-Wallis test (non parametric
578 1-way Anova), and a Dunn's *post hoc* test. * $p < 0.05$ and ** $p < 0.01$. ASC, antibody-secreting
579 cell.

580

581 **Supplementary Figure 1. Comparing the effects of different excess ODN on the cell**
582 **surface SA levels.**

583 Non-biotinylated CpG (A), CTRL (B) and INH (C) ODN were added in 10- and 100-fold
584 excess. Surface SA shows the anti-SA staining of the complexes on the cell surface. The
585 concentration of SA-CpG was 50 nM for BMDC and 25 nM for spleen cells. Cells were
586 harvested 24 h after stimulation and analyzed by flow cytometry. CD45R⁺ lymphocyte-sized
587 cells were considered B cells, CD45R⁻ lymphocyte-sized cells were considered T cells, I-A/I-

588 E⁺ cells were considered BMDC. The diagrams show mean + SD of at least four independent
589 experiments, normalized to the SA treatments. The treatments containing excess ODN were
590 compared to the SA-CpG treatment. Statistical differences were assessed by pairwise
591 comparisons of relevant groups using permutation tests, *p<0.05. Anti-SA antibody control
592 (D): levels of total and surface SA after labeling spleen B cells with SA on ice, using an anti-
593 CR1/2 scFv-SA complex. The diagrams show mean + SD of two independent experiments,
594 normalized to the SA treatments. No statistical significance was calculated. RFI, relative
595 fluorescence intensity.

596

597 **Supplementary Figure 2. Relative mRNA expression of TLR9 in non-activated and**
598 **activated BMDC, B cells and T cells.**

599 After 24 h of incubation with or without CpG (50 nM CpG for BMDC and 25 nM CpG for
600 spleen cells) BMDC were positively separated from BM culture with anti-mouse CD11c
601 magnetic microbeads or biotinylated anti-mouse I-A/I-E and anti-biotin magnetic microbeads.
602 Spleen suspension was separated to CD19⁺ (B cell) and CD19⁻ (T cell) populations with anti-
603 mouse CD19 magnetic beads. RNA was extracted and converted to cDNA for quantitative
604 real-time PCR analysis. Variations in cDNA input were normalized using $\beta 2m$ (Applied
605 Biosystems) as a reference gene and the expression level of TLR9 in B and T cells was
606 calculated as the *n*-fold difference relative to the expression found in BMDC. Each dot depicts
607 technical parallels and horizontal lines indicate their mean. Representative results of three
608 independent experiments are shown.

609 **Table 1. Name and composition of vaccines.**

Name	Composition
SA	SA-MycHH-biotin (in IFA)
SA + CpG	SA-MycHH-biotin + CpG (in IFA)
SA-CpG	SA-MycHH-biotin-CpG-biotin (in IFA)
SA-CpG + CpG	SA-MycHH-biotin-CpG-biotin + CpG (in IFA)
SA-CTRL	SA-MycHH-biotin-CTRL-biotin (in IFA)
SA-INH	SA-MycHH-biotin-INH-biotin (in IFA)

610

611 Each treatment contained 5 µg (83.3 pmol) SA/mouse, and all other components in equimolar
612 ratios. In the case of SA-CpG + CpG the total amount of ODN was 83.3 pmol. Each treatment
613 contained 75 µl IFA/mouse. The prime and the boost vaccine contained the same materials in
614 the same amounts.

615 SA, streptavidin;

616 MycHH, biotinylated Myc-tag HexaHis tag peptide;

617 CpG, CpG motif containing ODN 1668;

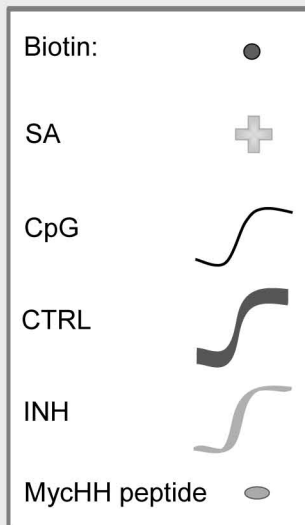
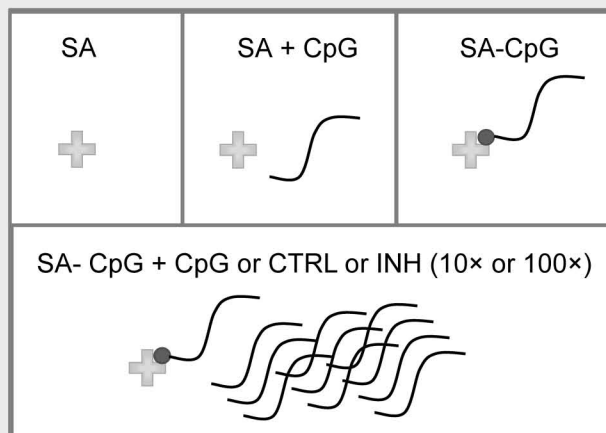
618 CTRL, ODN 1720 that contains the CG basepair of the CpG motif of ODN 1668 in reverse
619 order;

620 INH, ODN 2088 that binds to but inhibits activation of TLR9;

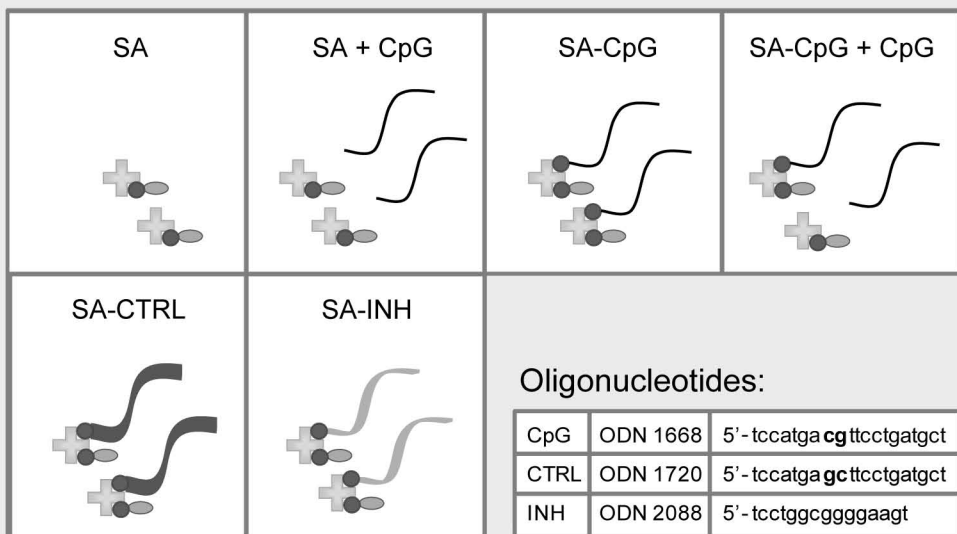
621 IFA, incomplete Freund's adjuvant.

Figure 1.

Composition of in vitro treatments:



Composition of vaccines:



Oligonucleotides:

CpG	ODN 1668	5' - tccatga cg ttctgatgct
CTRL	ODN 1720	5' - tccatga gc ttctgatgct
INH	ODN 2088	5' - tctggcggggaagt

Labeling of cells:

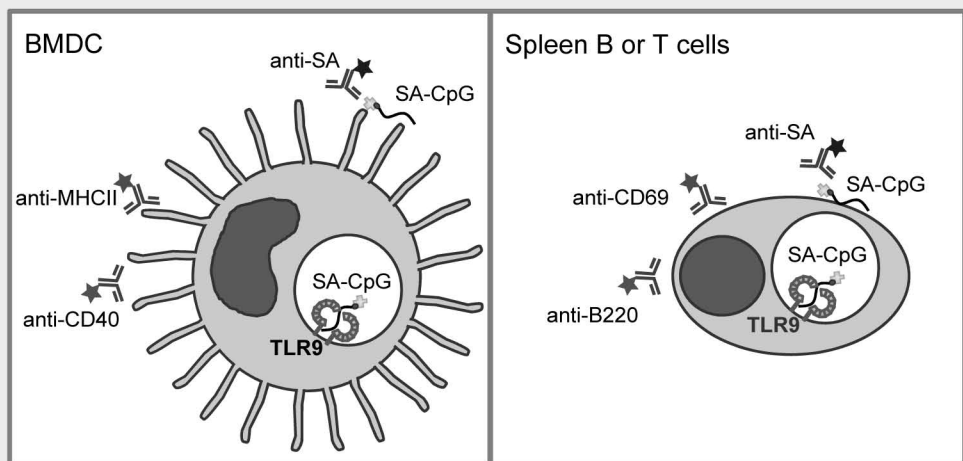


Figure 2.

BMDC

B cell

T cell

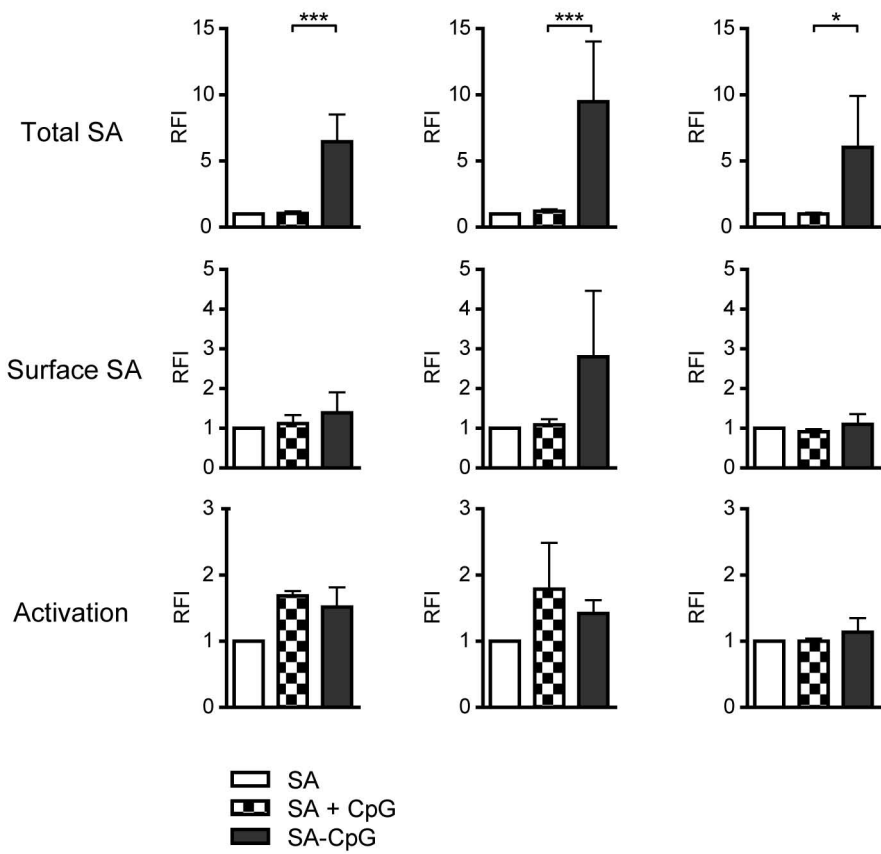


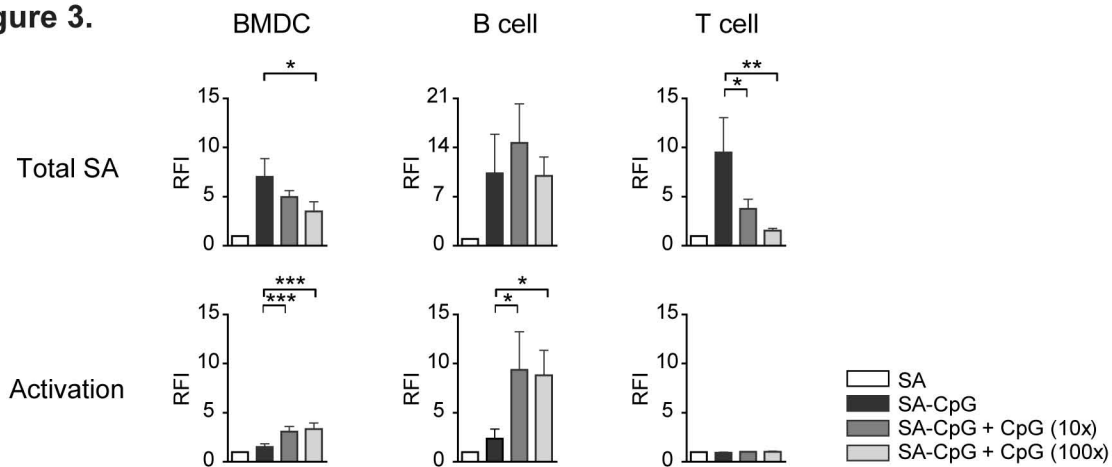
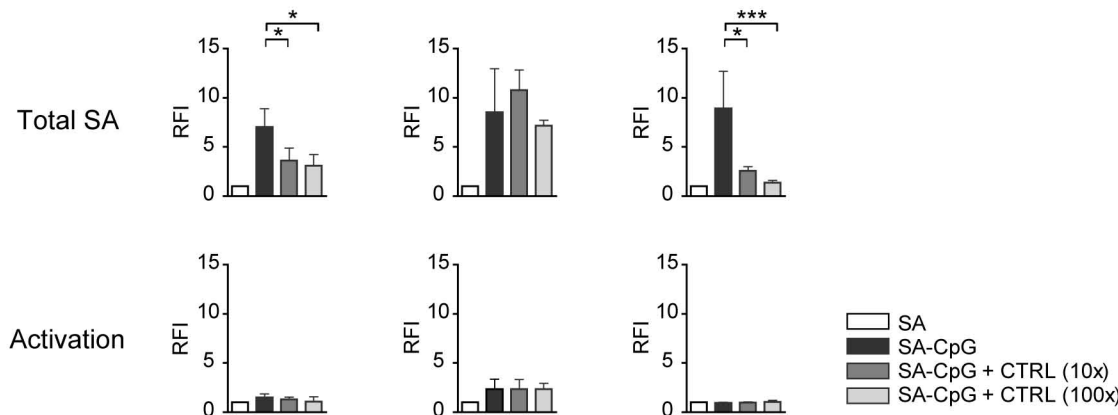
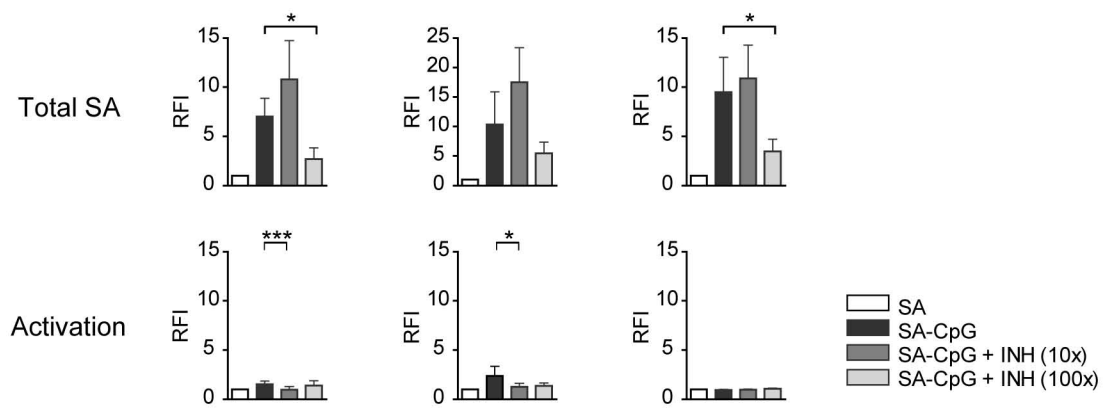
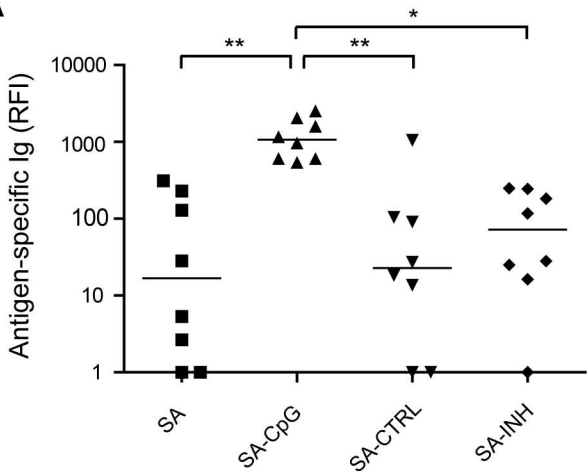
Figure 3.**A****B****C**

Figure 4.

A



B

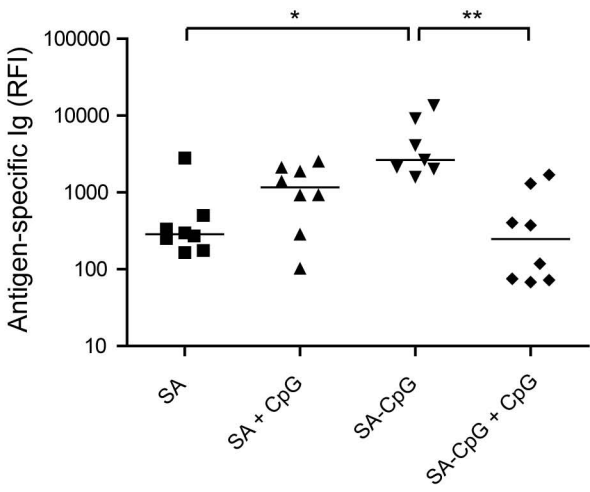
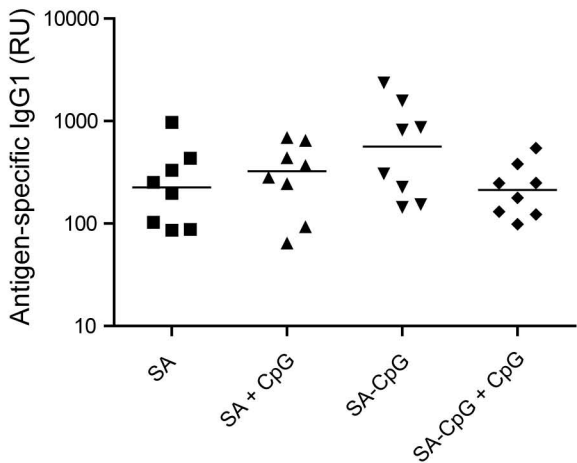


Figure 5.

A



B

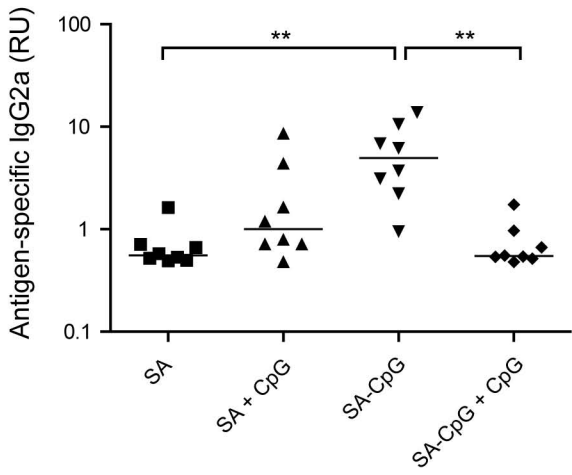
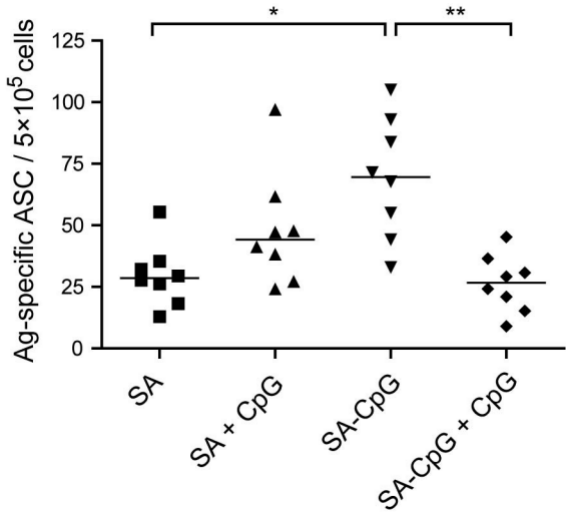
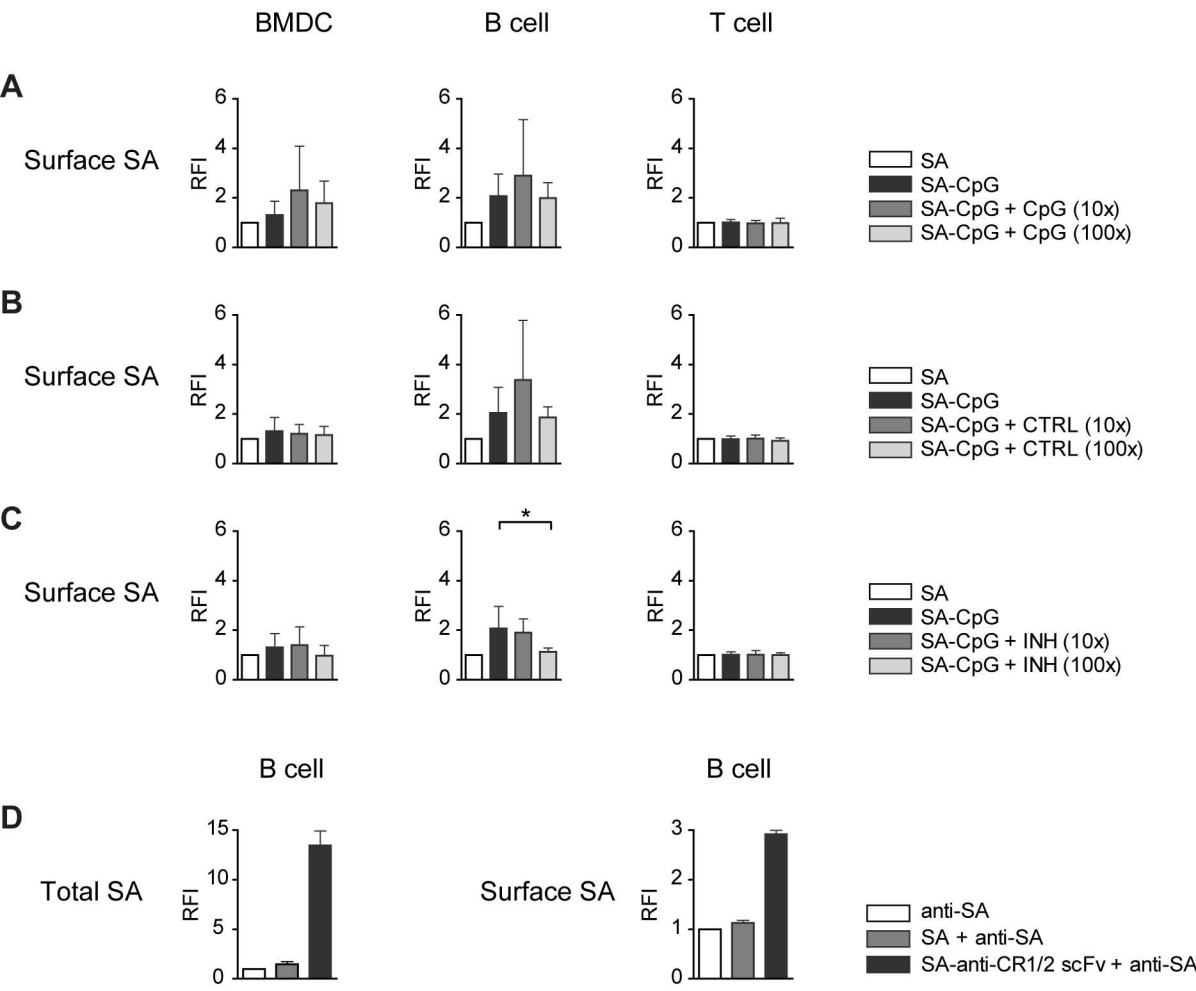


Figure 6.



Supplementary Figure 1.



Supplementary Figure 2.

